JOURNAL OF VIROLOGY, Oct. 2006, p. 9402–9413 Vol. 80, No. 19
0022-538X/06/$08.00+0 doi:10.1128/JVI.01086-06

Invasion of Host Cells by JC Virus Identifies a Novel Role for Caveolae in Endosomal Sorting of Noncaveolar Ligands†

W. Querbes,[1] B. A. O'Hara,[2] G. Williams,[2] and W. J. Atwood[1,2]*

Graduate Program in Pathobiology[1] and Department of Molecular Biology, Cell Biology, and Biochemistry,[2] Brown University, Providence, Rhode Island 02912

Received 26 May 2006/Accepted 6 July 2006

Invasion of glial cells by the human polyomavirus, JC virus (JCV), leads to a rapidly progressing and uniformly fatal demyelinating disease known as progressive multifocal leukoencephalopathy. The endocytic trafficking steps used by JCV to invade cells and initiate infection are not known. We demonstrated that JCV infection was inhibited by dominant defective and constitutively active Rab5-GTPase mutants that acted at distinct steps in endosomal sorting. We also found that labeled JCV colocalized with labeled cholera toxin B and with caveolin-1 (cav-1) on early endosomes following internalization by clathrin-dependent endocytosis. JCV entry and infection were both inhibited by dominant defective mutants of eps15 and Rab5-GTPase. Expression of a dominant-negative scaffolding mutant of cav-1 did not inhibit entry or infection by JCV. A single-cell knockdown experiment using cav-1 shRNA did not inhibit JCV entry but interfered with a downstream trafficking event important for infection. These data show that JCV enters cells by clathrin-dependent endocytosis, is transported immediately to early endosomes, and is then sorted to a caveolin-1-positive endosomal compartment. This latter step is dependent on Rab5-GTPase, cholesterol, caveolin-1, and pH. This is the first example of a ligand that enters cells by clathrin-dependent endocytosis and is then sorted from early endosomes to caveosomes, indicating that caveolae-derived vesicles play a more important role than previously realized in sorting cargo from early endosomes.

The human polyomavirus JC virus (JCV) infects 70% of the population worldwide and is responsible for the fatal central nervous system demyelinating disease progressive multifocal leukoencephalopathy (4, 11). This disease is rare and typically occurs in patients with impaired T-cell immunity. Recently, the development of progressive multifocal leukoencephalopathy has been associated with specific therapies designed to inhibit leukocyte trafficking into inflamed tissue (10, 12, 25).

The early events in infection of cells by JCV have been described in some detail. JCV interacts initially with α(2-6)-linked sialic acid and then subsequently binds to the 5-HT2a receptor to mediate cellular entry (8, 14). Following receptor interactions, the virus enters cells by clathrin-dependent endocytosis (21, 22). JCV infection is inhibited by drugs that block the clathrin-mediated pathway as well as by dominant defective mutants of a key component of clathrin pit formation, eps15 (3, 21, 22). Ligands, such as simian virus 40 (SV40), BK virus, and cholera toxin B (CT-B) use caveola-dependent endocytosis and are not affected by these drugs or by eps15 mutants (7, 18, 22). In addition to clathrin- and caveola-mediated endocytosis, some ligands can also enter cells by caveolae and clathrin-independent mechanisms (9).

Following clathrin-dependent endocytosis, ligands, including viruses, are generally trafficked to early endosomes and then sorted to recycling endosomes or to a late-endosomal/lysosomal compartment (1, 5). Early endosomes are highly dynamic organelles with a mosaic of diverse domains on the endosomal membrane regulating the proper trafficking of cargo (20). The trafficking of cargo along the endosomal/lysosomal pathways as well as through many other cellular organelles is regulated by the Rab-family GTPases. Rab5 serves as a key organizer of early events and also is involved in the transport of early endosomes along microtubules (17, 18, 23, 24). The Rab11 GTPase is segregated into membrane domains on endosomes that are required for sorting cargo to recycling endosomes (24). The Rab7 GTPase associates with distinct membrane domains from Rab11 and is involved in sorting of cargo toward the late endosome/lysosome pathway (2). Endosomal microdomains expressing different combinations of Rab proteins have distinct biochemical compositions and pharmacological properties that are required to properly sort different cargo to different sites within the cell (23). Viruses and bacteria have evolved multiple mechanisms allowing them to traffic through and eventually escape from these endosomal compartments.

To understand the trafficking events involved in JCV infection, we used dominant defective mutants of several key proteins involved in cellular trafficking. By comparing and contrasting the internalization of JCV to the internalization of two ligands of caveola-mediated endocytosis, SV40 and CT-B, we describe a novel cellular pathway used by JCV to infect cells. We conclude that JCV enters cells by clathrin-dependent endocytosis followed by a novel Rab5-dependent pathway from early endosomes to caveolae-derived vesicles. This work suggests that cross talk between different cellular transport mechanisms can provide for diverse intracellular pathways that are exploited by microorganisms.

* Corresponding author. Mailing address: Department of Molecular Biology, Cell Biology, & Biochemistry, Brown University, 70 Ship Street, Box G-E434, Providence, RI 02903. Phone: (401) 863-3116. Fax: (401) 863-9653. E-mail: Walter_Atwood@Brown.edu.

† Supplemental material for this article may be found at http://jvi.asm.org/.

MATERIALS AND METHODS

Cells, virus, and antibodies. SVG-A cells are a subclone of the original SVG human glial cell line established by transformation of human fetal glial cells by an origin-defective SV40 mutant (15). SVG-A cells were cultured in Eagle's

minimum essential medium (Mediatech, Inc.) supplemented with 10% heat-inactivated fetal bovine serum and kept in a humidified 37°C CO_2 incubator. The generation and propagation of the Mad-1/SVEΔ strain of JCV has been described previously (13, 14). As JCV does not form plaques on any cell type, our input multiplicities of infection are based on the number of DNA-containing particles contained in one hemagglutination unit (HAU). We have carefully measured this in the lab using standard and accepted practices in the field and have determined that 512 HAU per 1×10^5 cells is equivalent to a multiplicity of infection of 10.0. JCV was purified by sucrose density centrifugation followed by cesium chloride gradient centrifugation as previously described (22). For labeling, purified JCV was dialyzed against labeling buffer (0.1 M sodium bicarbonate, pH 8.0) and incubated for 1 h at room temperature with 0.1 mg of Alexa Fluor labeling dye according to the manufacturer's instructions (Molecular Probes). The labeled virus was then dialyzed against two exchanges of fresh buffer A (10 mM Tris, pH 8, 50 mM NaCl, 0.01 mM $CaCl_2$). Viral titers were determined by hemagglutination and infectivity assays, and the coupling ratio was determined according to the manufacturer's instructions. SV40 strain 776 was propagated in the African green monkey kidney cell line CV-1. The PAB597 hybridoma was used as a source of the anti-V antigen monoclonal antibody. The hybridoma was a gift from Ed Harlow, and the antibody recognizes both JCV and SV40 V antigen. The monoclonal antibody, PAB962, is specific for JCV T antigen and was a gift from Satvir Tevethia (Penn State College of Medicine). Generation of JCV and SV40 polyclonal antiserum has been previously described. Other antibodies used were against early endosomal antigen 1 (EEA1) (BD Biosciences), anti-golgin-97 (Molecular Probes), anti-caveolin-1 (anti-cav-1), and anti-calregulin (Santa Cruz Biotechnology). Secondary Alexa Fluor-labeled antibodies were from Molecular Probes.

Indirect immunofluorescent analysis. SVG-A cells grown on coverslips were infected with virus (either JCV or SV40) at a multiplicity of infection of 10. At 48 and 72 h postinfection, cells were washed in phosphate-buffered saline (PBS) and fixed in either ice-cold acetone for 10 min or in 4% paraformaldehyde for 30 min, followed by Triton-X permeabilization. Coverslips were stained with PAB597 or PAB962 for 45 min at 37°C. The coverslips were then washed and incubated with goat anti-mouse Alexa Fluor 488 (Molecular Probes) diluted in PBS. Cells were washed three times, and in some cases, counterstained with 0.02% Evan's blue. The coverslips were then mounted onto slides with fluorescence mounting media. (Vector Laboratories, Inc.). Slides were viewed using an epifluorescence microscope (Eclipse E800; Nikon, Inc.) and scored by counting. A minimum of eight fields were counted using the 20× objective for each experimental sample, and all experiments were repeated at least 3 times.

Confocal microscopy/constructs. Green fluorescent protein (GFP)-Rab constructs GFP-Rab5, GFP-Rab7, GFP-Rab11, GFP-Rab5-S34N, GFP-Rab7-T22N, and GFP-Rab11-S25N were kind gifts of Stephen Furguson (Robart Research Institute) and Craig Roy (Yale University). The wild-type and F92A-V94A Myc-tagged caveolin-1 constructs were generous gifts from M. J. Quon (National Institutes of Health). The GFP-eps15 constructs D3Δ2, DIII, and E95/295 were a generous gift from A. Benmerah (Institut Pasteur). The Rab5-Q79L mutant was generated with the QuikChange site-directed mutagenesis kit from Stratagene. SVG-A cells grown on coverslips were transfected with the indicated constructs for 24 h using FuGENE transfection reagent (Roche) prior to treatment with drugs, ligands, or labeled virus as indicated. Cells were then washed in PBS two times and fixed in 4% paraformaldehyde for 30 min. Coverslips were then mounted onto slides with mounting media (Vector Laboratories) and visualized by laser-scanning confocal microscopy using a 63× objective (LSM 410; Zeiss, Inc.).

For infection inhibition experiments using dominant defective mutants, cells were transfected with 2.0 μg of each dominant defective Rab-GFP construct using FuGENE transfection reagent (Roche) for 24 h in serum-free Eagle's minimum essential medium. At 24 h posttransfection, when GFP expression was maximal, cells were infected with 514 HAU of Alexa Fluor 594-labeled JCV or with 514 HAU of unlabeled JCV for 4 h at 37°C. For infection experiments, cells were fixed in paraformaldehyde and permeabilized in 0.05% Triton-X, and the indirect immunofluorescence assay for virus infection was carried out as described above except that the secondary antibody was labeled with Alexa Fluor 594 (red). For Rab-GFP confocal experiments, infected cells were washed in PBS and fixed with 4% paraformaldehyde for 30 min. In cases where antibody staining was done, cells were permeabilized with 0.2% saponin and quenched with 50 mM ammonium chloride. Cells were then washed with PBS again and mounted onto coverslips using fluorescent mounting media (Vector Laboratories). Slides were visualized by laser-scanning confocal microscopy using a 63× objective (LSM 410; Zeiss, Inc.). All images were analyzed using Adobe Photoshop.

Western blotting/density gradient centrifugation. SVG-A cells grown in 150-cm^2 flasks were infected with 514 HAU of JCV at 4°C for 30 min to allow binding and then shifted to 37°C for the indicated times to allow entry. Cells were then washed in cold PBS and lysed in ice cold radioimmunoprecipitation assay buffer (20 mM Tris HCl, pH 7.4, 0150 mM NaCl, 1% NP-40, 0.25% sodium deoxycholate, 1 mM EDTA, 1 mM phenylmethylsulfonyl fluoride, protease inhibitor cocktail [Sigma-Aldrich], 1 mM sodium orthovanadate). In cell fractionation experiments, lysates were disrupted by Dounce homogenization and sonication, and the nuclei and cellular debris were pelleted. The supernatants were layered at the bottom of a 40%–30%–5% discontinuous Optiprep gradient. Gradients were centrifuged at 34,000 rpm overnight in a swinging bucket ultracentrifuge, and nine 400-μl fractions were collected form the top of the gradient by pipetting. Proteins were transferred to nitrocellulose membranes using a mini-*trans* blot apparatus (Bio-Rad) and blocked with 1× casein blocking buffer (Sigma). Blots were probed with the respective antibodies all diluted in 1× blocking buffer, washed in PBS containing 0.05% Tween 20, and then incubated with goat anti-rabbit Alexa Fluor 680 (Molecular Probes) antibody diluted 1:5,000 in blocking buffer, followed by further washes with PBS-Tween 20 and once in PBS. Blots were viewed using an infrared scanner (LICOR) and analyzed using Odyssey software.

shRNA single-cell knockdown of cav-1. Short hairpin RNA (shRNA) was designed to target the specific sequences of caveolin-1 (GAGCTTCCTGATTG AGATT)-CVA and (CAAGGCCATGGCAGACGAG)-CVB and cloned into the RNAi-Ready pSIREN-RetroQ-ZsGreen vector from BD Biosciences. SVG-A cells were transfected with cav-1 shRNAs or with a control shRNA targeting luciferase (LUC) using Fugene transfection reagent (Roche). Seventy-two hours posttransfection, when cav-1 protein levels were reduced, cells were challenged with either 514 HAU of JCV or 4.8×10^6 PFU of SV40, which corresponds to a multiplicity of infection of approximately 10 for each virus. Infection was scored by staining for the viral protein T antigen and counting the percentage of shRNA-expressing cells that were infected. These values were then expressed as a percentage of the control (shRNA against luciferase).

RESULTS

JCV infection is dependent on Rab5 but not Rab7 or Rab11. SVG-A cells were transfected with wild-type and mutant GFP-tagged versions of Rab5, Rab7, and Rab11 GTPases and then challenged with virus in a single-cell infection assay. Only the dominant defective Rab5-GTPase (Rab5S34N) interfered with JCV infection (Fig. 1a). Cells transfected and expressing dominant defective Rab 7-GTPase or Rab 11-GTPase were equally susceptible to JCV infection, indicating that JCV does not need to traffic to recycling endosomes or to a late endosomal/lysosomal compartment for productive infection to occur (Fig. 1a). To determine if JCV associated with domains containing GFP-tagged Rab-GTPases, we performed colocalization experiments using Alexa Fluor 594-labeled JCV with each of the wild-type Rab-GFP proteins. Labeled JCV only colocalized with Rab5-GFP (GFP-Rab5) (Fig. 1b). No colocalization was seen between labeled JCV and either Rab7-GFP or Rab11 GFP (data not shown). As expected, expression of the dominant defective Rab5-S34N-GFP mutant reduced viral entry into cells and subsequent colocalization with Rab5 (Fig. 1c).

As a control, we tested each of the wild-type and mutant GFP-tagged Rab-GTPases for their ability to localize properly in the cell and to block endosomal trafficking of known ligands. Each mutant behaved as expected (see Fig. S1 in the supplemental material).

A caveolae-to-early endosome pathway in SVG-A cells. Productive infection of SVG-A cells does not require Rab7 or Rab11 GTPases. This indicates that JCV does not use the pathway from early endosomes to either late endosomes/lysosomes or recycling endosomes to infect cells. A novel pathway that traffics CT-B from caveolae to early endosomes and the Golgi has been described and we wanted to determine whether this pathway was functional in SVG-A cells (16, 18). We found

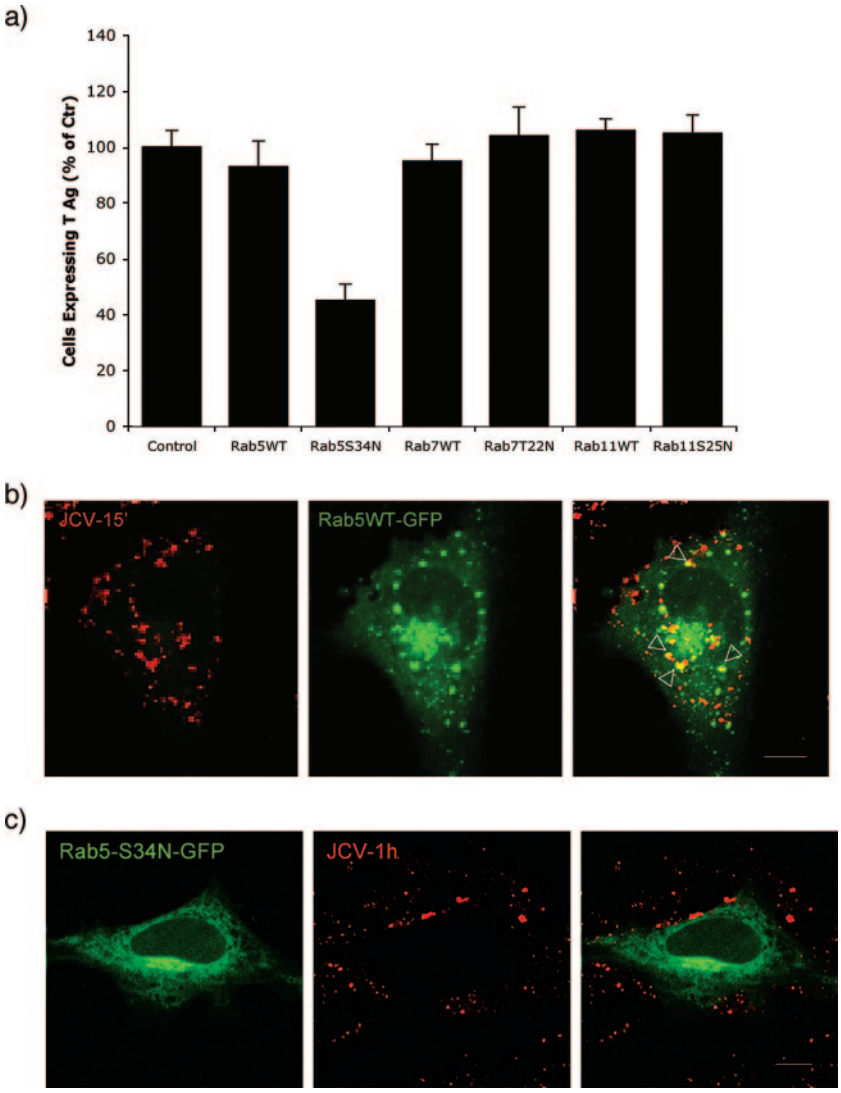

FIG. 1. Role of Rab GTPases in JCV infection. (a) Effects of Rab GTPases on JCV infection. SVG-A cells grown on coverslips were transfected with GFP-Rab5, GFP-Rab7, GFP-Rab11, GFP-Rab5S34N, GFP-Rab7T22N, or GFP-Rab11S25N. Twenty-four hours posttransfection, cells were infected with 512 HAU of JCV. At 48 h postinfection, cells were fixed and stained for the early viral protein T antigen. The fraction of Tag-expressing cells of at least 150 transfected cells from three different experiments was determined and presented as a percentage of that of the nontransfected control cells. (b) A representative cell showing colocalization of Alexa Fluor 594-labeled virus (JCV-15′) with GFP-Rab5 (Rab5WT-GFP). Cells were viewed by confocal microscopy using a 63× objective. The merged signal is shown in the far right panel (yellow). (c) The Rab5-S34N mutant (Rab5-S34N-GFP) blocks Alexa Fluor 594-labeled virus (JCV-1h) entry into cells. Bars, 10 μm.

that labeled CT-B colocalized with caveolin-1 within 10 min of exposure, by 30 min, labeled CT-B colocalized with a marker of early endosomes, EEA1, and by 1 h, CT-B colocalized with a marker of the Golgi, Golin-97 (Fig. 2a; the red and green channels of the overlays shown in this figure are shown separately in Fig. S2a in the supplemental material).

To confirm that CT-B was getting to endosomes and the Golgi by clathrin-independent endocytosis, we transfected cells with an eps15 mutant and found that CT-B was transported to the Golgi by 1 h postexposure (Fig. 2b). To determine whether the trafficking of CT-B from caveolae to endosomes was regulated by Rab5, we transfected cells with the Rab5 dominant defective mutant (Rab5-S34N) and showed that CT-B was retained in caveolin-1-positive domains and failed to reach the Golgi (Fig. 2c). Expression of a caveolin-1 scaffolding mutant blocked internalization of CT-B into cells (Fig. 2d). These data demonstrated that CT-B entered SVG-A cells by caveola-mediated endocytosis, was transported in a Rab5-GTPase-dependent manner to early endosomal membranes, and subsequently trafficked to the Golgi.

Expression of the Rab5-Q79L mutant inhibits JCV infection. We next asked whether this pathway was bidirectional and possibly exploited by JCV to infect the cell. To address this, we transfected cells with the Rab5-Q79L constitutively active mutant and confirmed that this mutant caused endosomal fusion and the formation of enlarged early endosomes (Fig. 2e). Expression of this mutant has also been shown to cause shunting and docking of caveola-derived vesicles on

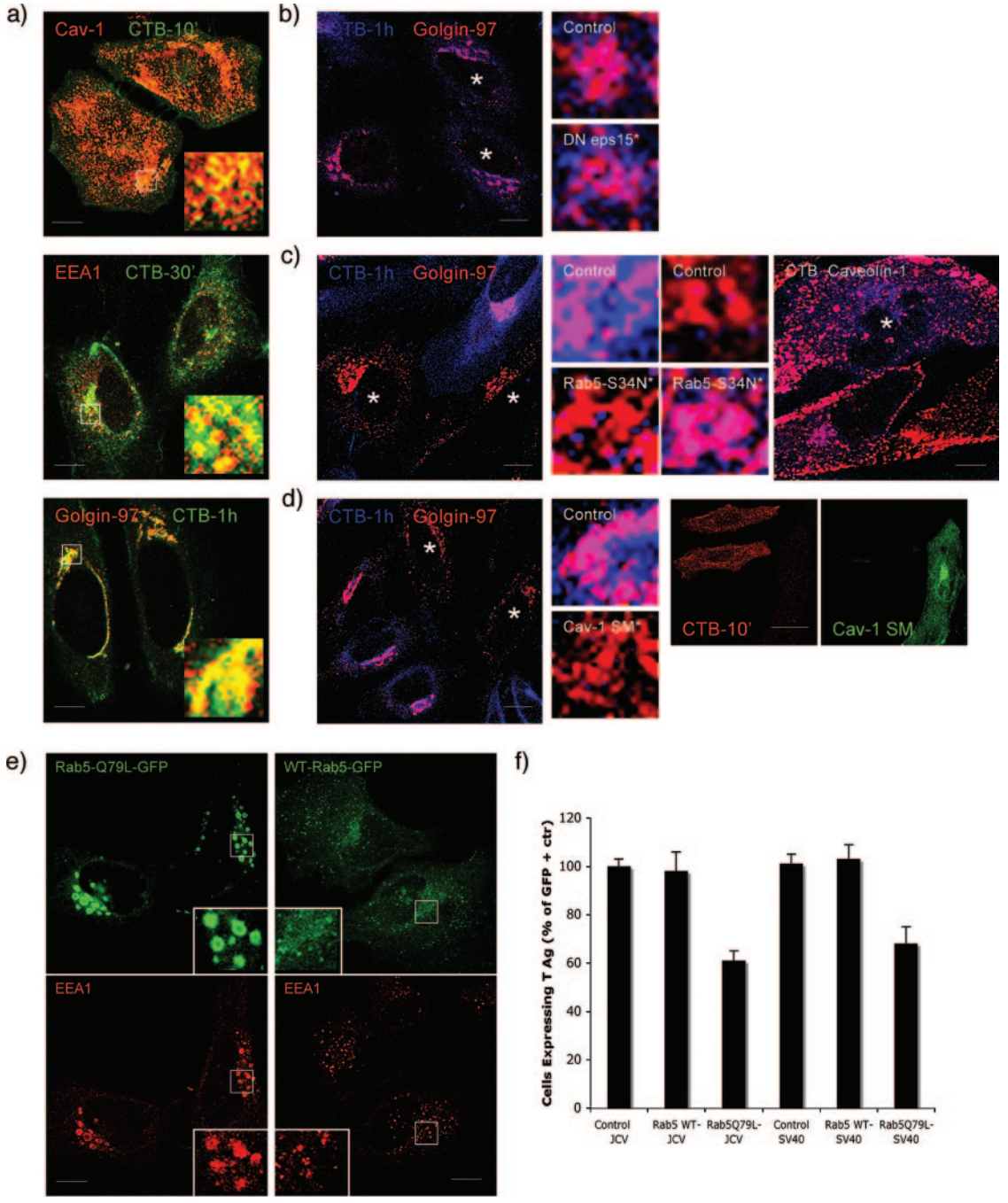

FIG. 2. A pathway of intracellular trafficking from caveolae to early endosomes exists in SVG-A cells and is exploited by JCV. (a) Trafficking of CT-B through the cell. SVG-A cells on coverslips were allowed to internalize 200 pg of Alexa Fluor 647-labeled CT-B for the indicated times at 37°C. Cells were then fixed and stained with antibodies to caveolin-1 (caveolae), EEA1 (early endosomes), and Golgin-97 (Golgi), followed by Alexa Fluor 594-labeled secondary antibodies. The merged yellow signal indicated colocalization of CT-B with caveolin-1 at 10 min (top), with EEA1 at 30 min (middle), and with Golgin-97 at 60 min (bottom). (b) CT-B does not enter cells by clathrin-dependent endocytosis. SVG-A cells were transfected with an eps15 mutant that blocks clathrin assembly and then exposed to CT-B for 1 h. When clathrin endocytosis is blocked, CT-B can still efficiently be trafficked to the Golgi, as seen by the merged (magenta) signal. Stars indicate cells expressing dominant defective eps15. Enlarged images of a control cell and an eps15-expressing cell are shown. (c) Rab5 is required for proper CT-B trafficking. SVG-A cells were transfected with the Rab5-S34N mutant for 24 h. Cells were then exposed to CT-B for 1 h, fixed, and then stained for Golgin-97 or caveolin-1. In cells expressing the Rab5-S34N mutant, CT-B is retained in caveolae and fails to accumulate in the Golgi. Stars indicate cells expressing dominant defective Rab5S34N. Images at right show that expression of Rab5S34N prevents CT-B from trafficking from caveolae to early endosomes. (d) CT-B does not enter cells expressing a caveolin-1 scaffolding mutant (cav-1 SM). SVG-A cells were transfected with a caveolin-1 scaffolding mutant for 24 h. Cells were then exposed to CT-B for 1 h, fixed, and then stained for Golgin-97. In cells expressing the caveolin-1 scaffolding mutant, CT-B was unable to efficiently enter cells, and none is seen in the Golgi or even to enter the cell by 1 h. Stars indicate cells expressing a scaffolding mutant of caveolin-1. Panels at right indicate that CT-B fails to enter cells expressing the cav-1 scaffolding mutant. (e) Expression of the Rab5Q79L mutant causes endosomal fusion and the formation of enlarged endosomes. SVG-A cells on coverslips were transfected with the Rab-Q79L mutant for 24 h. Cells were then fixed and stained for the early endosomal antigen EEA1, followed by Alexa Fluor 594 secondary antibodies. (f) Expression of the Rab5-Q79L mutant inhibits JCV infection. SVG-A cells on coverslips were transfected with the Rab-Q79L mutant for 24 h and then infected with either JCV or SV40. Forty-eight hours postinfection, cells were fixed and stained for the early viral protein T antigen. The results are plotted as a percentage of nontransfected control cells from three independent experiments. Bars, 10 μm.

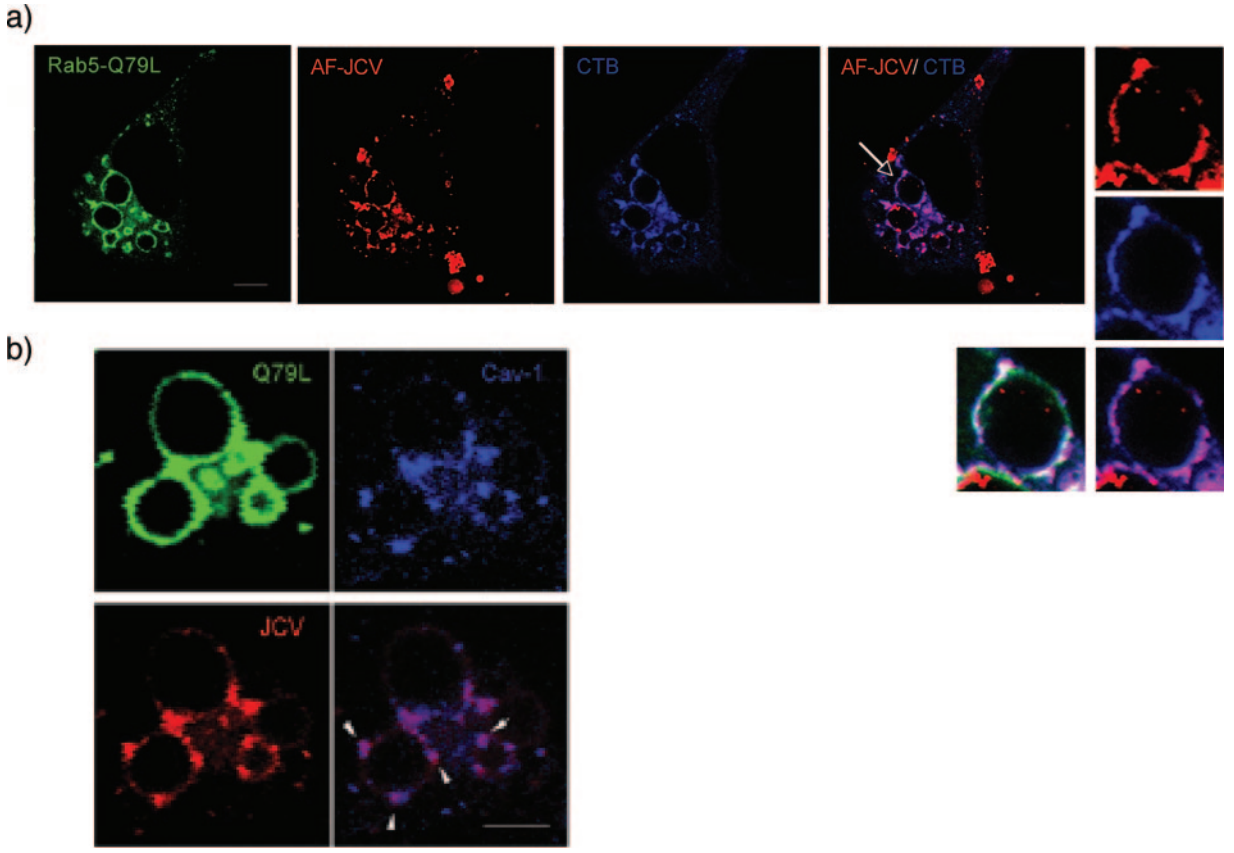

FIG. 3. Labeled JCV colocalizes with CT-B and cav-1 in domains on Rab5-Q79L enlarged endosomes. (a) SVG-A cells on coverslips were transfected with Rab5-Q79L-GFP for 24 h. Cells were then exposed to Alexa Fluor 594-labeled JCV (red) for 1 h at 4°C to synchronize binding, followed by a 1-h shift to 37°C to allow virus internalization. The cells were then exposed to Alexa Fluor 647-labeled CT-B (blue) for 15 min. Cells were fixed and viewed via laser-scanning confocal microscopy. JCV colocalizes with CT-B (magenta) in the same domains on the Rab5-Q79L enlarged endosomes. Bars, 10 μm. (b) SVG-A cells grown on coverslips were transfected with Rab5-Q79L for 24 h, exposed to labeled JCV (red) for 30 min, and then fixed and stained for caveolin-1(blue). The panels at the right show that JCV colocalizes with caveolin-1 in patches on endosomal membranes (arrow). Bars, 5 μm.

early endosomes that can disrupt the normal trafficking of ligands, such as SV40, along the caveolae-caveosome pathway (18). We found that expression of the Rab5Q79L mutant reduced infection of SVG-A cells by both JCV and SV40 (Fig. 2f). These data led us to hypothesize that JCV may traffic from early endosomes to caveosomes.

Labeled JCV, but not other markers of clathrin-dependent endocytosis, associates with CT-B and cav-1 on endosomal membranes. To determine whether JCV localized with CT-B on early endosomes, we transfected cells with the GFP-Rab5Q79L mutant and then exposed cells to Alexa Fluor 594-labeled JCV. The Rab5Q79L mutant causes fusion and enlargement of early endosomes, allowing for easy visualization of the early endosomal membrane. When we performed a colocalization experiment in cells expressing Rab5-Q79L, labeled JCV, and labeled CT-B, we found that JCV and CT-B colocalized in CT-B-containing domains on early endosomes (Fig. 3a). In the same experiment, we also demonstrate that labeled JCV colocalizes with caveolin-1 on these same endosomal domains (Fig. 3b). Note that JCV associates with early endosomes under normal conditions as shown in Fig. 1b.

To determine the specificity of this interaction, other ligands were tested for their ability to localize with CT-B-containing domains in Rab5-Q79L-transfected cells. Rab5-Q79L-transfected cells were exposed to labeled CT-B, to the clathrin-dependent ligand transferrin, or to the fluid phase marker dextran. When analyzed by confocal microscopy, we found that CT-B clearly associated with specific domains on Rab5-Q79L endosomal membranes but that transferrin and dextran accumulated inside the lumen of enlarged endosomes (Fig. 4). This suggests that not all ligands that enter cells by clathrin-dependent endocytosis or by other means use CT-B-containing domains on endosomes for trafficking, and this is most likely a unique event specific to some ligands and exploited by JCV.

An early event in JCV infection following entry is sensitive to cholesterol disruption. As caveolar function is disrupted by the cholesterol-sequestering drug MβCD, we sought to determine whether MβCD could inhibit JCV infection. We found that pretreatment of SVG-A cells with MβCD reduced JCV infection (Fig. 5a). Infection was partially restored by the addition of exogenous cholesterol (Fig. 5a). Note that treatment of cells with MβCD did not inhibit clathrin-dependent endocytosis of transferrin, indicating that the effect of MβCD was down-

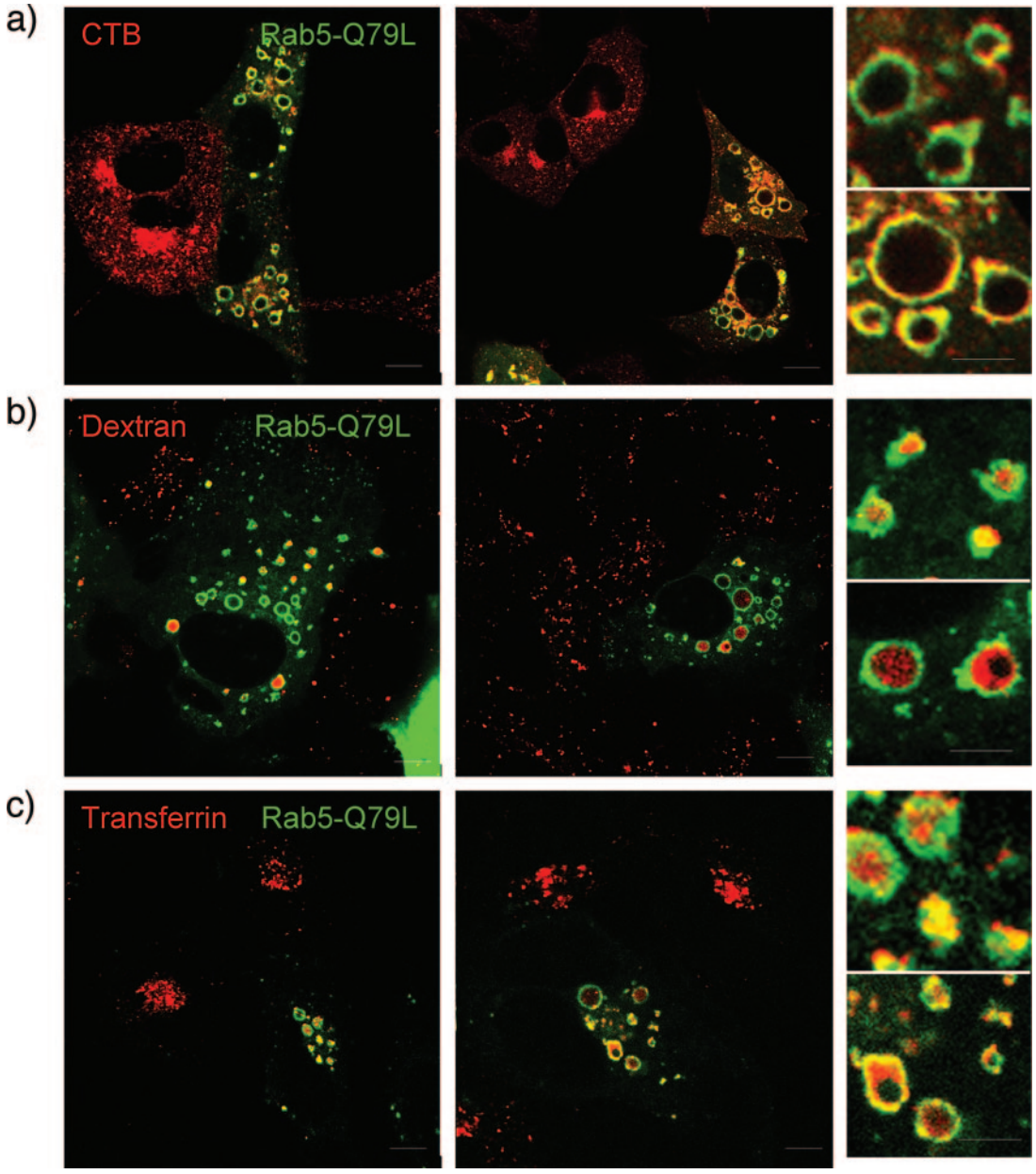

FIG. 4. CT-B localizes in distinct domains on the outside of Rab-5-Q79L endosomes. SVG-A cells on coverslips were transfected with Rab5-Q79L for 24 h. Cells were then exposed to Alexa Fluor 594-labeled CT-B (a marker of caveolae-dependent endocytosis) (a), dextran (a marker of clathrin-dependent endocytosis) (b), or transferrin (a marker of clathrin-dependent endocytosis) (c). Cells were fixed and viewed by laser-scanning confocal microscopy with a 63× objective. Ligands that use clathrin-dependent endocytosis (dextran and transferring) are trafficked to early endosomes and accumulate in the lumen of Rab5-Q79L enlarged endosomes. A marker of caveolae-dependent endocytosis, CT-B, localizes to distinct domains around the outside of the enlarged Rab5-Q79L endosomes. The small boxes at right are enlargements of individual endosomes. Bars, 10 μm.

stream of virus entry (see Fig. S3 in the supplemental material). To determine when during the course of JCV infection the drug was acting, we performed a time course experiment where the drug was added to cells before or at various times following virus exposure. We found that MβCD reduced infection when added up to 20 min following virus internalization, suggesting that the drug affected a step downstream of clathrin-dependent endocytosis which occurs within 10 min (21) (Fig. 5b). To further show that MβCD was inhibiting a step downstream of virus binding and entry, we performed a Triton X-100 wash-out experiment. Labeled JCV was bound to SVG-A cells at 4°C and then shifted to 37°C. The cells were then washed with Triton X-100 immediately or at 5, 10, 30, and 60 min following the shift to 37°C. Labeled virus was completely washed-out of the cells at the 0-, 5-, and 10-min time points (Fig. 5c). Labeled virus could not be washed out at either 30 min or at the 1-h time point, indicating that the virus does not interact with the Triton-insoluble membrane mi-

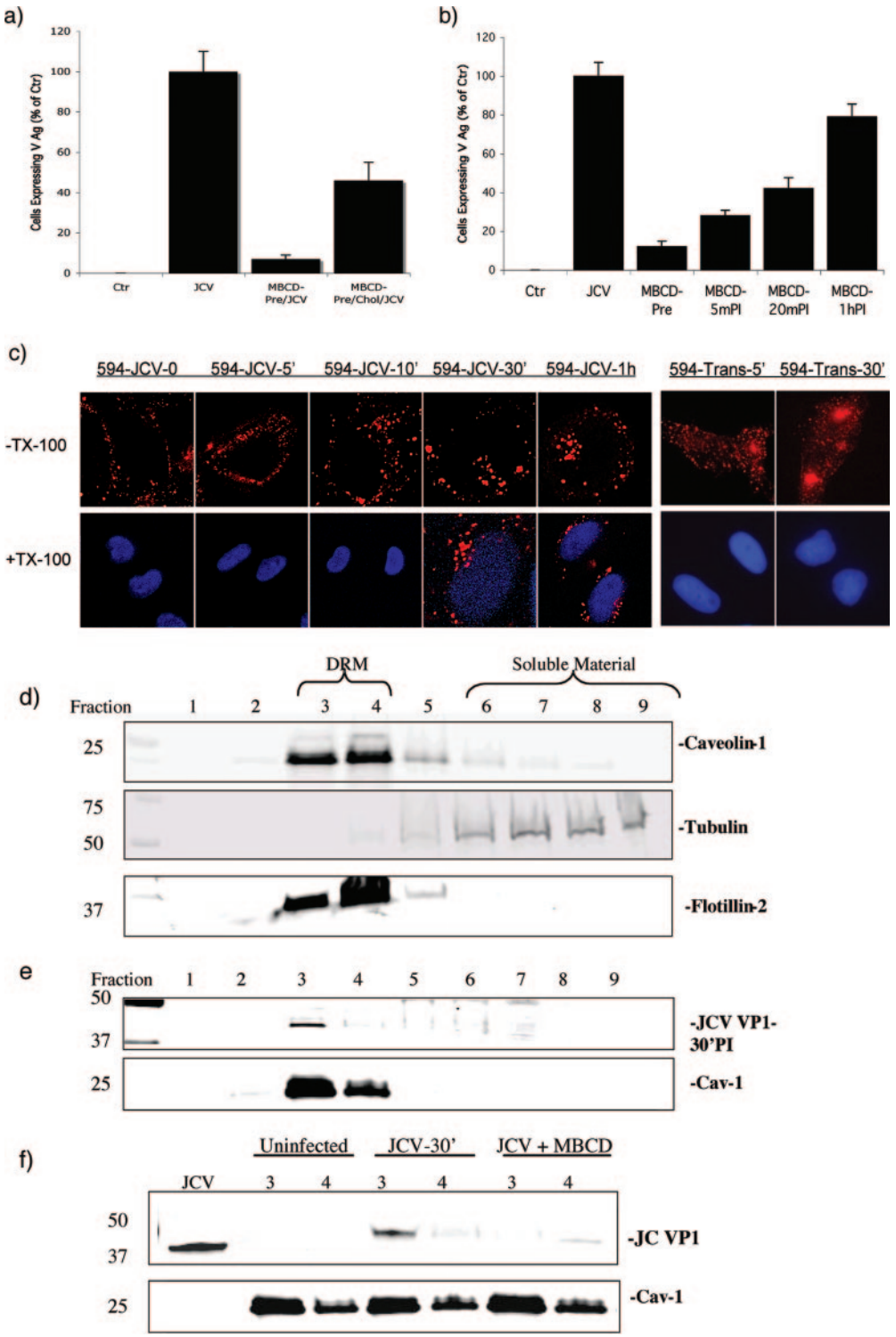

FIG. 5. The early events in JCV infection are dependent on cholesterol. (a) Pretreatment of SVG-A cells with the cholesterol-sequestering drug MβCD reduced JCV infection, and addition of exogenous cholesterol partially restored the ability of JCV to infect MβCD-treated cells. (b) MβCD was added before or at the indicated times postinfection (PI). MβCD was inhibitory when added up to 20 min postinfection, indicating that the drug affected a postentry step. (c) Alexa Fluor 594-labeled JCV (594-JCV) or Alexa Fluor 594-labeled transferrin (594-Trans) was allowed to internalize into SVG-A cells for the indicated times. The cells were then washed in Triton X-100, and the distribution of labeled virus or transferrin was visualized by confocal microscopy. Triton X-100 washed out the transferrin label at all time points tested, indicating that transferrin does not associate with Triton X-100-insoluble membrane microdomains. In contrast, JCV was found to enter a Triton X-100-resistant compartment by 30 min postentry. (d) Isolation of low-density, Triton X-100-insoluble membrane microdomains. Membrane microdomains were isolated from SVG-A cells by density gradient centrifugation. Fractions were taken by pipetting from the top of the gradient and subjected to Western blotting with antibodies specific for rafts/caveolae (caveolin-1/flotilin) or soluble material (tubulin). The membrane microdomains float to low-density fractions

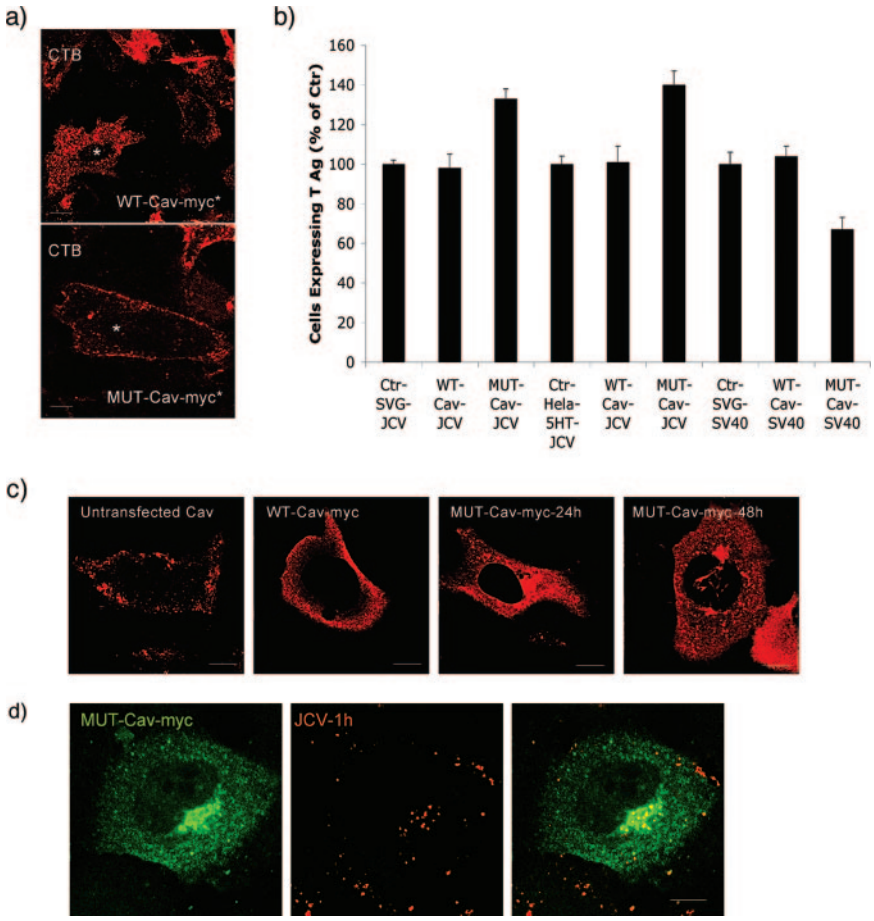

FIG. 6. A caveolin-1 scaffolding domain mutant does not inhibit entry or infection of cells by JCV. (a) Cells were transfected with a WT myc-tagged caveolin-1 construct (WT-Cav-myc) or with a Myc-tagged scaffolding mutant of cav-1 (MUT-Cav-myc), then exposed to Alexa Fluor 594-labeled CT-B (CT-B) for 30 min, and viewed by confocal microscopy. Only the scaffolding mutant blocked entry of CT-B, whereas the wild type had no effect. (b) Expression of the caveolin-1 mutant inhibits infection by SV40 and modestly enhances infection by JCV. SVG-A or HeLa-5HT cells were transfected with the cav-1 scaffolding mutant or with the wild-type construct. At 24 h posttransfection, cells were infected with JCV or SV40, and infection was scored at 48 h in Myc-expressing cells by staining with anti-T antigen antibodies. The percentage of Myc-positive cells expressing T antigen is expressed as a percentage of untransfected controls. (c) The caveolin-1 mutant has impaired plasma membrane localization. Antibody staining for cav-1 (left panel), Myc in WT-cav-1-transfected cells (second from left), or Myc in cells transfected with the scaffolding mutant (right two panels) is shown. In untransfected cells or in cell overexpressing the WT cav-1, the majority of the cav-1 is localized to the plasma membrane. The scaffolding mutant is not expressed at the plasma membrane and remains in the cytosol, as expected. (d) Alexa Fluor 594-labeled JCV (JCV-1h) can enter cells expressing the cav-1 scaffolding mutant. Bars, 5 μm.

crodomains on the cell surface but rather interacts with these domains at a postentry step (Fig. 5c). The clathrin-dependent endocytic ligand transferrin does not associate with Triton-insoluble membrane microdomains and it was completely washed out by Triton X-100 at both 5 min and 30 min post-adsorption (Fig. 5c).

We next biochemically confirmed that JCV associated with detergent-resistant membrane microdomains that could be disrupted by MβCD. To do this, JCV was bound to cells at 4°C and then shifted to 37°C for 30 min. The cells were lysed then layered at the bottom of a 40%–30%–5% density gradient. Fractions were collected from the top of the gradient and analyzed by Western blotting. We found that JCV associated with a low-density Triton-insoluble compartment in fractions 3 and 4 and cofractionated with known lipid raft markers and caveolin-1 (Fig. 5d and e). Furthermore, pretreatment of cells with MβCD blocked the association of JCV with the low-density Triton-insoluble domains (Fig. 5f).

3 and 4, whereas soluble material is found in the more highly dense fractions, primarily 7 to 9. (e) JCV localizes to a low-density membrane microdomain in fractions 3 and 4. The same experiment performed for panel d, except cells were first incubated for 1 h at 4°C with JCV and then shifted to 37°C for 30 min prior to cell lysis. (f) MβCD effects on JCV localization to the microdomains. The same experiment as done for panel e with the exception that some cells were pretreated with MβCD and only fractions 3 and 4 are shown, A lane containing just virus was used as a control. Treatment with MβCD disrupts the association of JCV with the low-density Triton-insoluble microdomain fractions 3 and 4.

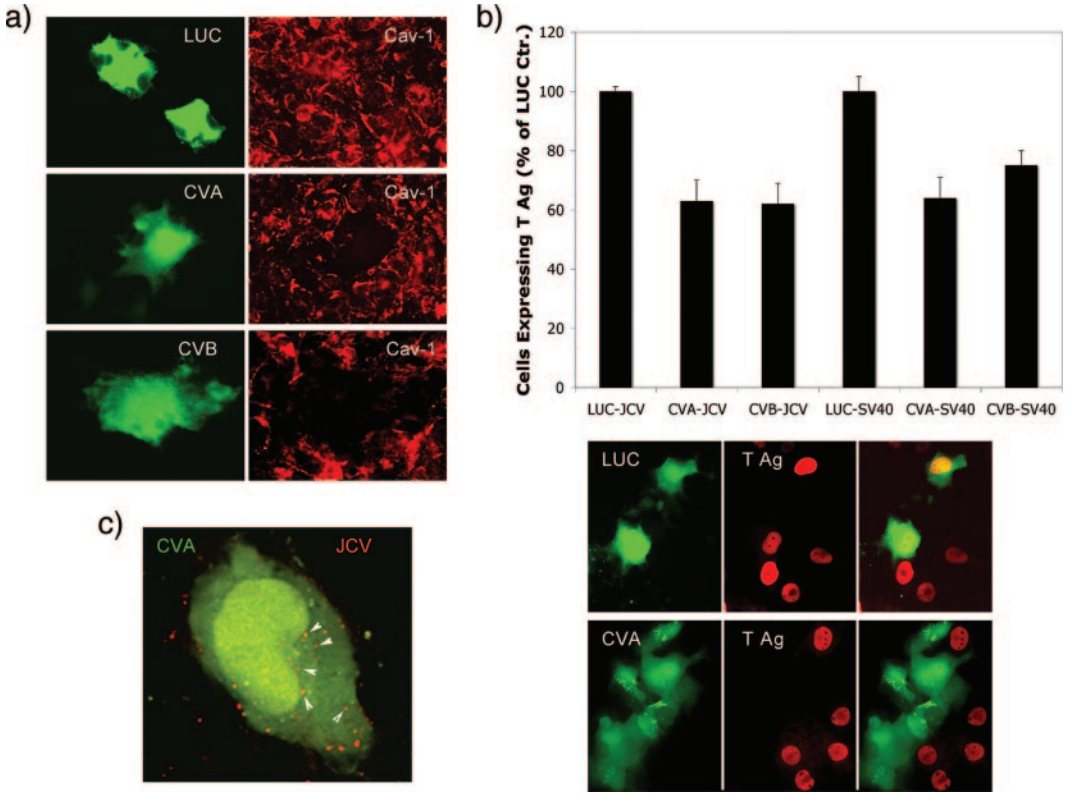

FIG. 7. Caveolin-1 single-cell knockdown inhibits JCV infection. (a) Cells were transfected with GFP-tagged constructs expressing either luciferase shRNA (LUC) or two shRNA constructs targeting caveolin-1 (CVA and CVB). At 72 h posttransfection, cells were stained with antibodies to caveolin-1 to assess the extent of knockdown (red). Both CVA and CVB diminished cav-1 protein expression, while the LUC control had no effect. (b) Cells were transfected with the same three shRNA constructs for 72 h and then exposed to either JCV or SV40. Infection was scored by examining viral T antigen expression in cells expressing the shRNAs. Representative cells expressing the shRNAs (green) that were infected with JCV and then stained for the viral protein T antigen (red) are shown in the bottom of panel b. (c) Alexa Fluor 594-labeled virus (red) can efficiently enter cells expressing the cav-1 shRNAs, showing that knockdown of cav-1 does not inhibit JCV entry. (The red and green channels of the overlays shown in panel C are shown separately in Fig. S2a in the supplemental material.)

JCV infection is not inhibited by expression of a caveolin-1 scaffolding mutant. To further examine if caveola-derived vesicles played a role in JCV infection, we transfected cells with either the wild type (WT) or a scaffolding domain mutant of caveolin-1. Compared to the wild type, the mutant impaired internalization of CT-B and reduced infection of cells by SV40 (Fig. 6a and b). In contrast, this mutant did not inhibit internalization of labeled JCV and did not inhibit infection (Fig. 6b and d). Expression of the mutant instead caused a redistribution of caveolin-1 from the plasma membrane to the cytosol, and this was associated with a modest increase in infection by JCV (Fig. 6b and c).

Caveolin-1 single-cell knockdown inhibits JCV infection. Two independent shRNAs against cav-1 were designed (CVA and CVB), and both reduced the expression of caveolin-1 protein levels in individual cells following transfection (Fig. 7a). A control shRNA (LUC) did not inhibit caveolin-1 expression in transfected cells (Fig. 7a). Cells transfected with CVA, CVB, or LUC shRNA were then challenged with JCV and infection scored at 48 h postinfection using an antibody that was specific for JCV T antigen. Expression of both the CVA and CVB shRNA reduced JCV and SV40 infection (Fig. 7b). The LUC shRNA did not inhibit infection by either virus (Fig. 7b). The effect of cav-1 knockdown was not at the level of virus entry, as JCV entered cells transfected with both CVA and CVB shRNA (Fig. 7c; the red and green channels of the overlays shown in this figure are shown separately in Fig. S2b in the supplemental material). These results indicate that caveola-derived vesicles play a role in JCV infection at a step following entry but before virus early gene expression.

JCV traffics from caveola-derived vesicles docked on endosomes to caveosomes and the ER. To examine the downstream pathway of JCV infection, we monitored the trafficking of labeled JCV over the course of 16 h. We found that, by 2 h postentry, JCV (JCV-2 h) extensively colocalized with cav-1 in perinuclear compartments resembling caveosomes (Fig. 8a). As SV40 traffics from caveolae to the ER, we sought to determine whether JCV may also intersect with this compartment. Our first approach was to determine whether the drug brefeldin A, an inhibitor of the ARF1 GTPase, could inhibit JCV infection. We found that brefeldin A inhibited infection of SVG-A cells by both JCV and SV40, indicating that, like SV40, productive trafficking of JCV to the ER is dependent on the ARF1 GTPase (Fig. 8b). This indicates that these related viruses intersect the same intracellular pathways from their quite distinct modes of initial entry. To confirm that JCV trafficked to the ER, we exposed cells to labeled JCV for either 12 h or 16 h and examined the colocalization of the virus with the ER

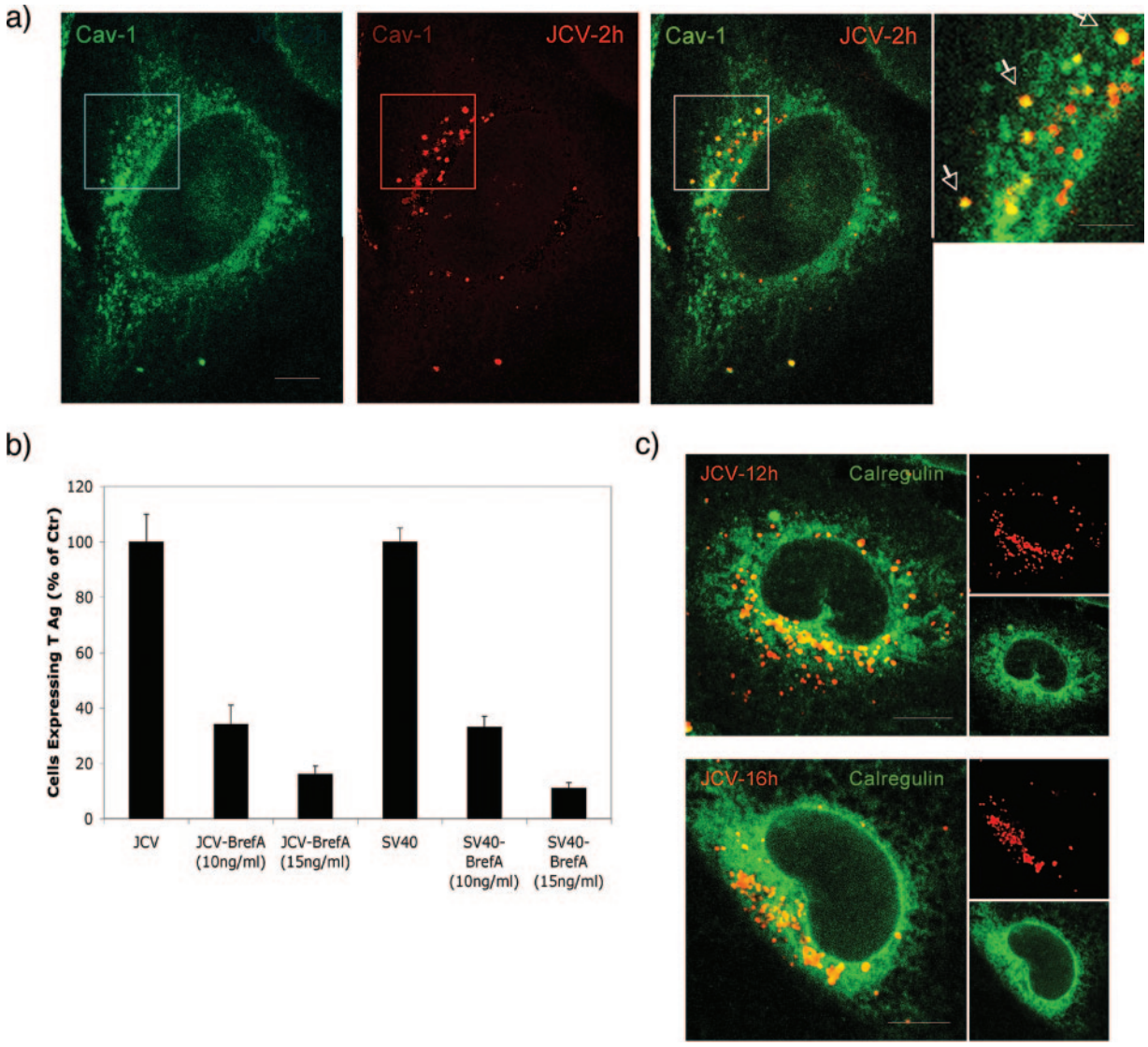

FIG. 8. JCV traffics from caveola-derived vesicles on early endosomes, to caveosomes, and then to the ER. (a) SVG-A cells were exposed to labeled JCV for 1 h at 4°C to allow binding and then for 2 h at 37°C to allow internalization. Cells were then fixed and stained for caveolin-1 (green). JCV colocalizes with caveolin-1 in caveosomes, as shown by the merged yellow signal (yellow). Bars, 10 μm. (b) Disruption of ER trafficking with brefeldin A (BrefA) inhibits both JCV and SV40 infection of SVG-A cells. Cells were infected with either JCV or SV40, treated with brefeldin A to disrupt the ER, and then fixed and stained for the earl viral protein T antigen 48 h postinfection. (c) JCV traffics to the ER. JCV was bound to cells at 4°C and then shifted to 37°C to allow internalization for either 12 or 16 h. Cells were then fixed and stained for the ER marker calregulin (green). By 12 h, some JCV colocalized with calregulin, but by 16 h, nearly all of the labeled JCV colocalized with calregulin. Bars, 10 μm.

marker, calregulin (calreticulin). We saw some colocalization at 12 h and significantly more colocalization by 16 h postentry (Fig. 8c). At these time points, JCV did not colocalize with Golgi or with lysosomal markers (not shown).

DISCUSSION

Understanding the mechanisms that viruses use to invade cells has given us a clearer picture of the diversity and complexity of normal cellular transport and sorting pathways. We provide evidence that JCV uses a novel pathway to infection that is both clathrin and caveolin-1 dependent and involves Rab5-GTPase-dependent sorting both to and from early endosomes. A Rab5 dominant defective mutant (Rab5-S34N) was the only dominant defective Rab-GTPase mutant tested that reduced JCV infection. These data are consistent with our earlier work showing that JCV entry and infection are inhibited by drugs and dominant defective mutants that specifically antagonize clathrin-dependent endocytosis (22). Drugs and dominant defective mutants that inhibit caveola-dependent endocytosis have no effect on JCV infection but do inhibit infection by SV40 and BK virus (7). We also show here that JCV initially resides in a Triton X-100-soluble compartment and becomes Triton X-100 insoluble only after it is endocytosed. This suggests that initial entry is clathrin dependent and caveolae and lipid raft independent. Additionally, wild-type Rab5 was

the only Rab-GTPase protein tested that colocalized with labeled JCV. Rab7 and Rab11 dominant defective mutants that blocked transport along the late-endosomal/lysosomal route and transport to recycling endosomes, respectively, had no effect on JCV infection, suggesting that JCV invasion did not follow either of these pathways.

A pathway of intracellular trafficking from caveolae to early endosomes has been previously described, and we show here that the pathway is intact in SVG-A cells and, more importantly, that it is bidirectional and exploited by JCV (16, 18). This pathway involves the transient docking of caveola-derived vesicles onto early endosomes. The caveola-derived vesicles do not fuse with the early endosome but rather retain their structure and release cargo, such as CT-B, into the endosomal membrane in a pH-dependent manner (18). This process is dependent on Rab5-GTPase, as a dominant defective Rab5-GTPase mutant (RabS34N) blocks CT-B transport to early endosomes by preventing caveola-derived vesicles from docking on the endosomes (18). A constitutively active mutant of Rab5-GTPase, Rab5Q79L, causes accumulation of caveola-derived vesicles docked on early endosomes. This mutant inhibits infection of SV40 by shunting internalized caveola-derived vesicles away from caveosomes and to early endosomes (18). When we expressed this mutant in cells that are permissive to JCV and SV40, we found that JCV infection was reduced to a level similar to that in SV40 infection. This suggested that JCV, which enters cells by clathrin-dependent endocytosis, also required caveola-derived vesicles for further trafficking. We also demonstrated that the association of JCV with cav-1 in the endosomal membranes is inhibited by treating cells with NH_4Cl, indicating that the reverse pathway from early endosomes to cav-1-containing compartments is also pH dependent (see Fig. S4 in the supplemental material). Our data on the Rab5 dependence of CT-B trafficking to the Golgi is consistent with that of Pelkmans et al. but differs from that of Nichols et al. (16, 18). This discrepancy may be due to the different cell types used in these studies.

To further define the role of early endosome-associated caveolae-derived vesicles in JCV infection, we transfected cells with a scaffolding mutant of caveolin-1. Expression of this mutant inhibited caveola-dependent endocytosis of CT-B and inhibited SV40 infection. In contrast, expression of this mutant did not inhibit infection by JCV but instead led to a modest enhancement of infection. We observed a redistribution of caveolin-1 in cells expressing the dominant-negative mutant and suggest that increased cytosolic levels of caveolin-1 can facilitate the intracellular sorting of ligands, such as JCV, from early endosomes to cav-1-containing compartments. These data also suggest that the process involved in docking of caveolin-1 at the plasma membrane and on endosomes is regulated differently. This is supported by data showing that caveolae-mediated endocytosis at the plasma membrane is a ligand-induced event, whereas docking and undocking of stable caveola-derived vesicles on endosomes occurs constitutively to promote proper endosomal sorting of ligands (6, 19).

Expression of the Rab5-Q79L mutant also caused endosomal fusion and the formation of enlarged endosomes, which made it possible to better visualize endosomes by confocal microscopy and examine where JCV localized following clathrin-dependent endocytosis. We found that labeled JCV localized to endosomal membrane domains and that other ligands that enter cells by clathrin-dependent endocytosis, such as transferrin, accumulated in the lumen of these endosomes. Furthermore, labeled JCV colocalized with CT-B and cav-1 in endosomal membrane domains, suggesting that they reside within the same compartment, most likely on docked caveola-derived vesicles.

As expression of a caveolin-1 scaffolding domain mutant enhanced JCV infection, we wanted to determine whether JCV required caveola-derived vesicles for productive infection by knocking down caveolin-1 using shRNA. Expression of two different shRNAs targeting cav-1 significantly knocked down caveolin-1 protein expression and reduced JCV infection. Importantly, expression of these shRNAs had no effect on the ability of the virus to enter cells, further validating that caveolin-1 and caveolae-derived vesicles play a role only after endocytosis of the virus. At time points of 1 h, we clearly saw JCV colocalize with caveolin-1 on enlarged endosomes, and by 2 h, we saw JCV colocalizing with caveolin-1 in perinuclear heterogeneously sized caveosomes. From there, labeled virus proceeded through a brefeldin A-sensitive transport pathway to the ER where, by 16 and 18 h, we saw strong colocalization with an ER marker, calregulin.

ACKNOWLEDGMENTS

We thank all members of the Atwood lab for critical discussions during the course of this work. We thank A. Benmerah, M. J. Quon, S. Ferguson, C. Roy, and P. Meneses for plasmids. We also thank Amanda Robinson, Amy Bozek, Tammy Glass, Wendy Virgadamo, and Lorie St. Pierre for administrative assistance.

Work in our laboratory was supported by a grant from the National Cancer Institute, R01 CA71878, and by a grant from the National Institute of Neurological Disorders and Stroke, R01 NS43097, to W.J.A. W.Q. is supported by a GAANN training grant from the Department of Education, P200A030100.

REFERENCES

1. **Bantel-Schaal, U., B. Hub, and J. Kartenbeck.** 2002. Endocytosis of adeno-associated virus type 5 leads to accumulation of virus particles in the Golgi compartment. J. Virol. **76:**2340–2349.
2. **Barbero, P., L. Bittova, and S. R. Pfeffer.** 2002. Visualization of Rab9-mediated vesicle transport from endosomes to the trans-Golgi in living cells. J. Cell Biol. **156:**511–518.
3. **Benmerah, A., M. Bayrou, N. Cerf-Bensussan, and A. Dautry-Varsat.** 1999. Inhibition of clathrin-coated pit assembly by an Eps15 mutant. J. Cell Sci. **112:**1303–1311.
4. **Berger, J. R., and E. O. Major.** 1999. Progressive multifocal leukoencephalopathy. Semin. Neurol. **19:**193–200.
5. **Bousarghin, L., A. Touze, P. Y. Sizaret, and P. Coursaget.** 2003. Human papillomavirus types 16, 31, and 58 use different endocytosis pathways to enter cells. J. Virol. **77:**3846–3850.
6. **Chen, Y., and L. C. Norkin.** 1999. Extracellular simian virus 40 transmits a signal that promotes virus enclosure within caveolae. Exp. Cell Res. **246:**83–90.
7. **Eash, S., W. Querbes, and W. J. Atwood.** 2004. Infection of Vero cells by BK virus is dependent on caveolae. J. Virol. **78:**11583–11590.
8. **Fonseca-Elphick, G., W. Querbes, J. A. Jordan, G. V. Gee, S. Eash, K. Manley, A. Dugan, M. Stanifer, A. Bhatnagar, W. K. Kroeze, B. L. Roth, and W. J. Atwood.** 2004. The human polyomavirus, JCV, uses serotonin receptors to infect cells. Science **306:**1241–1420.
9. **Kirkham, M., and R. G. Parton.** 2005. Clathrin-independent endocytosis: new insights into caveolae and non-caveolar lipid raft carriers. Biochim. Biophys. Acta **1745:**273–286.
10. **Kleinschmidt-DeMasters, B. K., and K. L. Tyler.** 2005. Progressive multifocal leukoencephalopathy complicating treatment with natalizumab and interferon beta-1a for multiple sclerosis. N. Engl. J. Med. **353:**369–374.
11. **Knowles, W. A., P. Pipkin, N. Andrews, A. Vyse, P. Minor, D. W. Brown, and E. Miller.** 2003. Population-based study of antibody to the human polyomaviruses BKV and JCV and the simian polyomavirus SV40. J. Med. Virol. **71:**115–123.

12. **Langer-Gould, A., S. W. Atlas, A. J. Green, A. W. Bollen, and D. Pelletier.** 2005. Progressive multifocal leukoencephalopathy in a patient treated with natalizumab. N. Engl. J. Med. **353:**375–381.
13. **Liu, C. K., and W. J. Atwood.** 2001. Propagation and assay of the JC virus. Methods Mol. Biol. **165:**9–17.
14. **Liu, C. K., G. Wei, and W. J. Atwood.** 1998. Infection of glial cells by the human polyomavirus JC is mediated by an N-linked glycoprotein containing terminal α(2-6)-linked sialic acids. J. Virol. **72:**4643–4649.
15. **Major, E. O., A. E. Miller, P. Mourrain, R. G. Traub, E. de Widt, and J. Sever.** 1985. Establishment of a line of human fetal glial cells that supports JC virus multiplication. Proc. Natl. Acad. Sci. USA **82:**1257–1261.
16. **Nichols, B. J., A. K. Kenworthy, R. S. Polishchuk, R. Lodge, T. H. Roberts, K. Hirschberg, R. D. Phair, and J. Lippincott-Schwartz.** 2001. Rapid cycling of lipid raft markers between the cell surface and Golgi complex. J. Cell Biol. **153:**529–541.
17. **Nielsen, E., F. Severin, J. M. Backer, A. A. Hyman, and M. Zerial.** 1999. Rab5 regulates motility of early endosomes on microtubules. Nat. Cell Biol. **1:**376–382.
18. **Pelkmans, L., T. Burli, M. Zerial, and A. Helenius.** 2004. Caveolin-stabilized membrane domains as multifunctional transport and sorting devices in endocytic membrane traffic. Cell **118:**767–780.
19. **Pelkmans, L., J. Kartenbeck, and A. Helenius.** 2001. Caveolar endocytosis of simian virus 40 reveals a new two-step vesicular-transport pathway to the ER. Nat. Cell Biol. **3:**473–483.
20. **Pfeffer, S.** 2003. Membrane domains in the secretory and endocytic pathways. Cell **112:**507–517.
21. **Pho, M. T., A. Ashok, and W. J. Atwood.** 2000. JC virus enters human glial cells by clathrin-dependent receptor-mediated endocytosis. J. Virol. **74:**2288–2292.
22. **Querbes, W., A. Benmerah, D. Tosoni, P. P. Di Fiore, and W. J. Atwood.** 2004. A JC virus induced signal is required for infection of glial cells by a clathrin- and eps15-dependent pathway. J. Virol. **78:**250–256.
23. **Sonnichsen, B., S. De Renzis, E. Nielsen, J. Rietdorf, and M. Zerial.** 2000. Distinct membrane domains on endosomes in the recycling pathway visualized by multicolor imaging of Rab4, Rab5, and Rab11. J. Cell Biol. **149:**901–914.
24. **Ullrich, O., S. Reinsch, S. Urbe, M. Zerial, and R. G. Parton.** 1996. Rab11 regulates recycling through the pericentriolar recycling endosome. J. Cell Biol. **135:**913–924.
25. **Van Assche, G., M. Van Ranst, R. Sciot, B. Dubois, S. Vermeire, M. Noman, J. Verbeeck, K. Geboes, W. Robberecht, and P. Rutgeerts.** 2005. Progressive multifocal leukoencephalopathy after natalizumab therapy for Crohn's disease. N. Engl. J. Med. **353:**362–368.